UNCLASSIFIED

SECURITY CLASSIFICATION OF THIS PAGE (When Data Entered)

REPORT DOCUMENTATION PAGE	READ INSTRUCTIONS BEFORE COMPLETING FORM
1. REPORT NUMBER: 13444.5-GS | 2. GOVT ACCESSION NO.: AD-A097 900	3. RECIPIENT'S CATALOG NUMBER: N/A
4. TITLE (and Subtitle): Thermal IR Exitance Model of a Plant Canopy	5. TYPE OF REPORT & PERIOD COVERED: REPRINT
	6. PERFORMING ORG. REPORT NUMBER: N/A
7. AUTHOR(s): D. S. Kimes, J. A. Smith, L. [illegible] Link	8. CONTRACT OR GRANT NUMBER(s): DAAG29-78-G-0045, DACW39-77-C-0013
9. PERFORMING ORGANIZATION NAME AND ADDRESS: Colorado State University, Fort Collins, CO 80523	10. PROGRAM ELEMENT, PROJECT, TASK AREA & WORK UNIT NUMBERS: N/A
11. CONTROLLING OFFICE NAME AND ADDRESS: US Army Research Office, PO Box 12211, Research Triangle Park, NC 27709	12. REPORT DATE: 15 Feb 81
	13. NUMBER OF PAGES: 10
14. MONITORING AGENCY NAME & ADDRESS (if different from Controlling Office)	15. SECURITY CLASS. (of this report): Unclassified
	15a. DECLASSIFICATION/DOWNGRADING SCHEDULE

16. DISTRIBUTION STATEMENT (of this Report)

Submitted for announcement only

17. DISTRIBUTION STATEMENT (of the abstract entered in Block 20, if different from Report)

18. SUPPLEMENTARY NOTES

19. KEY WORDS (Continue on reverse side if necessary and identify by block number)

20. ABSTRACT (Continue on reverse side if necessary and identify by block number)

New

412 258

DD FORM 1 JAN 73 1473 EDITION OF 1 NOV 65 IS OBSOLETE

UNCLASSIFIED

SECURITY CLASSIFICATION OF THIS PAGE (When Data Entered)

Reprinted from APPLIED OPTICS, Vol. 20, page 623, February 15, 1981

Thermal IR exitance model of a plant canopy

D. S. Kimes, J. A. Smith, and L. E. Link

A thermal IR exitance model of a plant canopy based on a mathematical abstraction of three horizontal layers of vegetation was developed. Canopy geometry within each layer is quantitatively described by the foliage and branch orientation distributions and number density. Given this geometric information for each layer and the driving meteorological variables, a system of energy budget equations was determined and solved for average layer temperatures. These estimated layer temperatures, together with the angular distributions of radiating elements, were used to calculate the emitted thermal IR radiation as a function of view angle above the canopy. The model was applied to a lodgepole pine (*Pinus contorta*) canopy over a diurnal cycle. Simulated vs measured radiometric average temperatures of the midcanopy layer corresponded within 2°C. Simulation results suggested that canopy geometry can significantly influence the effective radiant temperature recorded at varying sensor view angles.

I. Introduction

The thermal IR region (3–20 μm) of the electromagnetic spectrum may provide valuable information about the characteristics of natural or man-made targets. With the advent of satellite thermal sensor systems (e.g., the Heat Capacity Mapping Mission and the proposed Thematic Mapper on Landsat D as well as multispectral aircraft scanners), it is becoming more important to relate underlying scene phenomena to the remote sensing observables.[1] In both the design and utilization of electrooptical sensors it is important to be able to estimate the statistical characteristics of the target and background as a function of sensor parameters. Often empirical methods are used to obtain these required data.[2,3]

An alternative approach is to employ a physically based or process-oriented model of the scene.[4,5] This latter approach is particularly useful and often required when detailed or subtle characteristics of a target need to be enhanced.

Many thermal models exist for different nonvegetated targets of interest and for planar solid objects. For example, Watson[6] developed a thermal model for predicting the diurnal surface temperature variation of the ground, and the University of Michigan[7] developed a model for the prediction of time-dependent temperatures and radiance of planar targets and backgrounds. However, few thermal models exist for plant canopies; and in agriculture and forestry applications, vegetation is the primary target of interest.

Gates[8] presented an energy budget for a single plant leaf isolated in space, as did Kimes *et al.*[9] and Wiebelt and Henderson.[10] Other investigators have modeled the thermal dynamics of vegetation canopies assuming a simplistic single homogeneous layer abstraction. For example, vegetation was treated as a single homogeneous layer with an associated transmission factor for solar radiation in the University of Michigan model.[7] Heilman *et al.*[11] used thermal scanning data to measure crop effective radiant temperatures and used an evapotranspiration (ET) equation to estimate crop ET. They assumed that the sensor was viewing only the top layer of the crop, and they ignored the effects of canopy geometry on sensor response.

It is known that vegetation canopies are non-Lambertian at optical wavelengths primarily due to canopy geometry.[12] Similarly, in the thermal region, it is believed that while individual canopy elements are isotropic radiators, the response from the canopy may also be non-Lambertian, because canopy geometry causes spatial variations in many energy flow processes.

A primary objective of this paper is to describe a thermal IR exitance model of a plant canopy, which includes a detailed accounting of vegetation structure. The model was applied to a lodgepole pine canopy over a diurnal cycle. This treatment is then shown to result in angular variations in predicted thermal radiance.

D. S. Kimes is with NASA Goddard Space Flight Center, Earth Resources Branch, Greenbelt, Maryland 20771; J. A. Smith is with Colorado State University, Department of Forest & Wood Sciences, Fort Collins, Colorado 80523; and L. E. Link is with U.S.A.E. Waterways Experiment Station, Environmental Laboratory, Vicksburg, Mississippi 39180.

Received 7 March 1980.
0003-6935/81/040623-10$00.50/0.

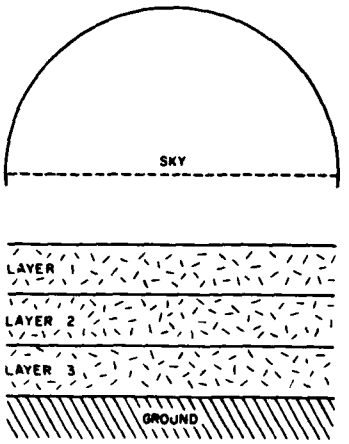

Fig. 1. Abstraction of the thermal canopy signature model (TCSM) showing the sky, ground, and three canopy layers which contain a statistical ensemble of elements.

II. Model Description

A description of the canopy abstraction and assumptions and canopy geometry will be presented followed by the energy budget equations for each layer, which account for the thermal radiation transfers, solar radiation absorption, thermal exitance, transpiration, and convection exchanges.

A. Canopy Abstraction and Assumptions

The vegetation canopy is abstracted as three, statistically independent, horizontal, infinite layers (Fig. 1). The canopy elements (e.g., leaves, branches, and other plant organs) within each layer are described as a statistical ensemble, which is used to define the canopy geometry. Midelements that represent canopy elements occurring in the middle of each layer are defined. An energy budget equation is formulated for the midelements of each layer. These equations account for the energy inflow and outflow processes of the midelements. The energy transfers are calculated on a power per unit area of element ($W \cdot m^{-2}$) basis. The roots of the resulting system of equations are the average surface temperature of the midelements in the three layers. It is assumed that these values represent the average temperature of the elements in each respective layer. These values are then utilized to calculate the response of a thermal sensor at varying view angles.

The flow of energy within a canopy is time-dependent. However, the model assumes a steady-state condition in which elements of the canopy are neither gaining nor losing a net amount of energy. In addition, the energy loss due to photosynthesis and energy gain by respiration is assumed negligible and has been ignored. Heat exchange by conduction is also considered negligible. These approximations are good for elements of relatively small dimensions[13]; but the steady-state and conduction assumptions may not be adequate when dealing with canopies that exhibit a large fraction of their total element surface areas as large branches and trunks. To approximate time-dependent events, one can consider a series of incremental changes in steady-state energy flow, as discussed later.

Several other assumptions are made. First, the spectral effects in the thermal region are assumed insignificant. Kondratyev[14] stated that natural surfaces can be treated in the first approximation as gray-body radiators and emitters. Data from Leeman *et al.*[15] showed that the thermal IR spectral emissivity of plants is essentially constant with wavelength.

Second, the reflection of thermal flux within the canopy is ignored. Ross[16] stated that the transfer theory for the thermal radiation in a vegetation canopy differs from shortwave theory in that the scattering of thermal radiation may be neglected, but the emission of thermal radiation from plant elements must be acknowledged. It is believed that within natural vegetation canopies reflected thermal radiation is a negligible contribution to the total energy budget. Blaxter[17] reported the emissivity of green grass as 0.99. Idso *et al.*[18] reported the emissivity of thirty-four plants ranging approximately from 0.94 to 1.00, with thirty plants above 0.96. A sensitivity analysis showed the effect of ignoring thermal reflectance on leaf temperature to be insignificant with reasonable ranges of plant emissivities.[19]

Finally, the individual canopy elements are assumed to emit thermal radiation in an isotropic manner. Kondratyev[14] and Hudson[20] stated that the radiation emitted from natural surfaces is essentially isotropic.

B. Canopy Geometry

Important parameters in describing radiation transfer in complex structures are the gap frequency and the extinction of radiation within the structure. Monteith,[21] Wilson,[22] de Wit,[23] and other authors have developed various formulas for these parameters. Nilson[24] presented a good review of these formulations for theoretical models of canopy geometry which have been utilized.

The mathematical structure of the model in this study is abstracted in the following manner to account for radiation transfers. Since the model is numerical as opposed to analytical in nature, the hemispheres above and below a particular layer are discretized into nine hemispherical inclination bands from 0 to 90° (Fig. 2). Each of the nine bands is further discretized into eighteen azimuthal sectors (Fig. 2). Within each sector the radiation transfers among the three canopy layers, ground, and sky are calculated.

The formulation developed by Idso and de Wit[25] has been incorporated to predict the probability of gap in the direction of the nine hemispherical bands for each of the three canopy layers. The positive binomial distribution is used to describe these probabilities, and azimuthal symmetry is assumed. The probability of gap in a particular band direction is equal to the ratio of the projection of planar elements in a layer to the projection of the underlying soil surfaces. For a hemispherical band direction j the equation is

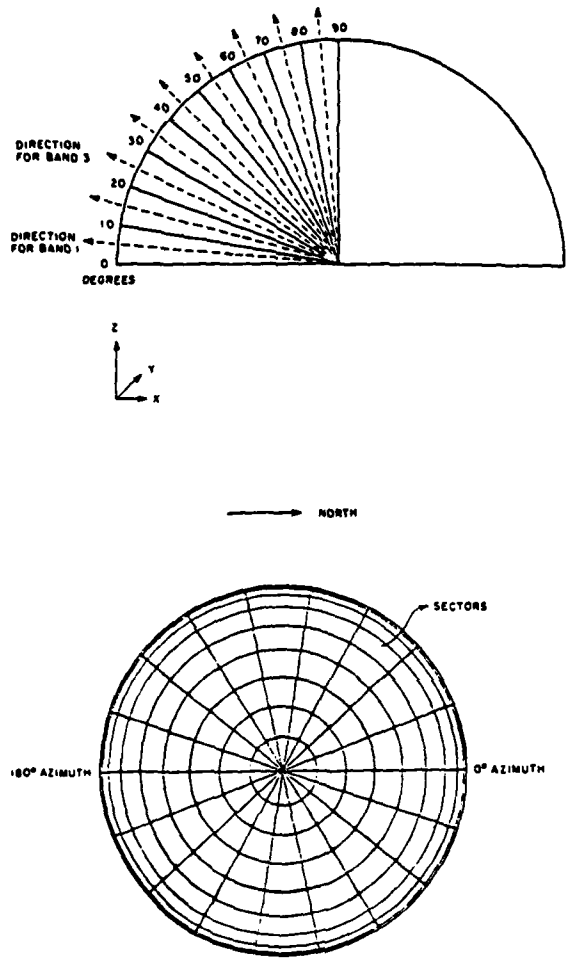

Fig. 2. Horizontal and vertical views of the nine hemispherical inclination bands which are divided into 18 equal azimuthal sectors. If one rotates the horizontal view about the axis the bands would occur in 3-D space.

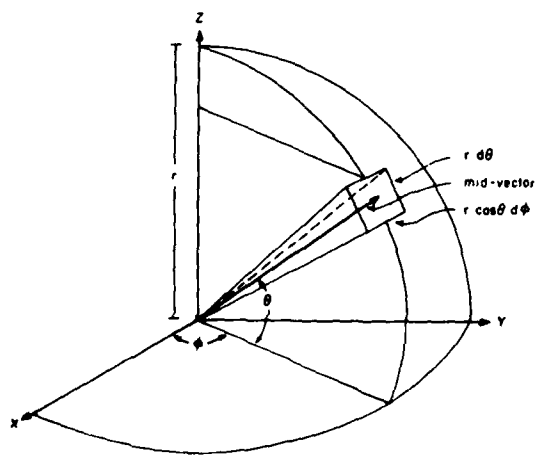

Fig. 3. Three-dimensional view of the solid angle represented by a particular sector with its corresponding midvector.

$$PGAP_{jm} = \left[1 - \frac{S_m \cdot G_{jm}}{\sin(\Theta_j)}\right]^{EAI_m/S_m}, \qquad PHIT_{jm} = 1 - PGAP_{jm},$$

where

$PGAP_{jm}$ = probability of gap for layer m in the direction of hemispherical band j;
$PHIT_{jm}$ = probability of hit for layer m in the direction of hemispherical band j;
G_{jm} = mean canopy projection of elements in layer m in the direction of hemispherical band j;
EAI_m = element area index for layer m;
S_m = index of spatial dispersion of elements in layer m; and
$\sin(\Theta_j)$ = sine function of the inclination angle Θ of hemispherical band j.

The function G_{jm} is determined from inclination angle frequency distributions of the elements in a layer. The derivation and computational procedure are presented by de Wit.[23] The parameter S_m ranges from 0 to 1 and is an index of denseness or spatial dispersion of the elements in a canopy. As S approaches 1.0, the more regular the dispersion of elements is and the less frequently a gap is encountered. The element area index of a canopy layer is equal to the ratio of the total one-sided element area within a layer to the area of the underlying soil area. For a more in-depth discussion of the above theory and the required measurements see Refs. 25 and 26.

The resulting $PGAP_{jm}$ and $PHIT_{jm}$ are important parameters in describing the radiation transfers within each hemispherical sector. In addition, the probabilities of gap and hit of half of each layer are required, and these parameters are calculated as

$$PGAP'_{jm} = (PGAP_{jm})^{1/2} \qquad PHIT'_{jm} = 1 - PGAP'_{jm},$$

where $PGAP'_{jm}$ is the probability of gap for one-half of layer m in the direction of hemispherical band j, and $PHIT'_{jm}$ is the probability of hit for one-half of layer m in the direction of hemispherical band j.

C. Thermal Radiation Transfers

Each layer emits and receives thermal radiation in the hemispheres occurring above and below a particular layer. The transfer of thermal radiation within each hemispherical sector between the three canopy layers, the sky, and ground is calculated as follows. As seen in Fig. 3, for small angles (Θ,ϕ) the two sides of a sector can be described as $r\cos\Theta d\phi$ and $rd\Theta$, and the area of the sector is described as $r^2\cos\Theta d\Theta d\phi$. One can then define the solid angle of a sector as

$$d\Omega = \frac{r^2\cos\Theta d\Theta d\phi}{r^2} = \cos\Theta d\Theta d\phi,$$

where Ω is the steradians of a sector. It follows that

$$\Omega = \int_{\phi_1}^{\phi_2}\int_{\Theta_1}^{\Theta_2} \cos\Theta d\Theta d\phi,$$

where ϕ_1 and ϕ_2 define the azimuthal limits of sector i in hemispherical band j, and Θ_1 and Θ_2 define the inclination limits of sector i in hemispherical band j.

To calculate the thermal irradiance on a planar mi-

delement from a particular layer in any given sector we proceed as follows. Assuming that canopy elements in a particular layer emit thermal radiation in an isotropic manner and have a homogeneous surface temperature and emissivity, the radiance $L(\mathrm{W \cdot m^{-2} \cdot sr^{-1}})$ from the material is

$$L = M/\pi, \tag{1}$$

where M is the exitance $(\mathrm{W \cdot m^{-2}})$.

The above radiance L is equal for all viewing directions; however, a canopy layer has special characteristics in that it is not solid but has gaps that are dependent on the direction of view. As a consequence, the irradiance on a midelement normal to the midvector (Fig. 3) of a relatively small sector is calculated by

$$E_{ij} = \int_{\phi_1}^{\phi_2} \int_{\Theta_1}^{\Theta_2} L \cdot \mathrm{PHIT}(\Theta) \cos\Theta d\Theta d\phi,$$

where E_{ij} is the irradiance $(\mathrm{W \cdot m^{-2}})$ on a midelement normal to the midvector from the sector i in hemispherical band j, L is the radiance of canopy elements from an infinite horizontal layer, and $\mathrm{PHIT}(\Theta)$ is the probability of hit for viewing angle Θ. The equations and theory of flux transfer from extended sources through solid angles to receiving elements are presented by the National Bureau of Standards.[27]

Assuming that $\mathrm{PHIT}(\Theta)$ is constant within sector ij,

$$E_{ij} = L \cdot \mathrm{PHIT}_j \int_{\phi_1}^{\phi_2} \int_{\Theta_1}^{\Theta_2} \cos\Theta d\Theta d\phi.$$

Because the eighteen sectors within band j have equal solid angles, the above equation can be reduced to

$$E_{ij} = \frac{L \cdot \mathrm{PHIT}_j}{18} \int_0^{2\pi} \int_{\Theta_1}^{\Theta_2} \cos\Theta d\Theta d\phi.$$

This expression can be further evaluated as

$$E_{ij} = L \cdot \mathrm{PHIT}_j \cdot \pi \frac{(\sin\Theta_2 - \sin\Theta_1)}{9}. \tag{2}$$

Combining Eqs. (1) and (2) for a particular sector and defining the quantity $(\sin\Theta_2 - \sin\Theta_1)/9$ as SECTOR_j, where j denotes the hemispherical band interval, the equation becomes $E_{ij} = M \cdot \mathrm{PHIT}_j \cdot \mathrm{SECTOR}_j$.

The above assumes that the midelement is normal to the direction of the source and that there exist no obstructions between the emitting canopy layer and the midelement. The following calculations correct for the fact that the panel or midelement is not always oriented normal to the source. The desired correction factor is the cosine of the angle between the source vector and the normal vector of the midelement. The theory is based on the existence of planar elements. The inclination angles of the canopy elements and source and the azimuthal angles of the leaves and source are discretized as before. The canopy elements are assumed to have azimuthal symmetry. The direction cosines of all source sectors are calculated as

$$\mathbf{V}_{ij} = \begin{bmatrix} \cos(\Theta_{ij})\cos(\phi_{ij}) \\ \cos(\Theta_{ij})\sin(\phi_{ij}) \\ \sin(\phi_{ij}) \end{bmatrix},$$

where $\mathbf{V}_{ij}$ is the vector of direction cosines for source sector i in hemispherical band j, and Θ_{ij} and ϕ_{ij} are the inclination and azimuth angle, respectively, of the midvector in sector i and hemispherical band j. When calculating the direction cosines of the normal vector of a midelement for each inclination angle interval, the azimuth angle is fixed to zero degrees since the canopy is assumed azimuthally symmetric, both in geometric and thermal radiant energy modes. Thus regardless of the azimuthal orientation of a midelement, the thermal radiant contributions to the midelement are constant for any specific inclination angle. The equation for the normal vectors is

$$\mathbf{N}_k = \begin{bmatrix} -\sin(\Theta_k) \\ 0.0 \\ \cos(\Theta_k) \end{bmatrix},$$

where $\mathbf{N}_k$ is the direction cosines of the normal vector of a planar element with inclination k, and Θ_k is the midelement inclination of k. The problem of a source sector hitting either the front or back side of a midelement is treated as presented by Oliver and Smith.[26]

Now one can calculate the absolute value of the dot products for all source–element angle permutations. These values are equal to the correction factors desired: $\mathrm{COS}_{ijk} = |\mathbf{V}_{ij}| \cdot |\mathbf{N}_k|$, where COS_{ijk} is the correction factor desired for permutations of source sector i in hemispherical band j and element inclination k. Applying this correction factor and the absorption coefficient for thermal radiation, the equation becomes

$$(\phi_{ijk})/\mathrm{m^2} = M \cdot \mathrm{PHIT}_j \cdot \mathrm{SECTOR}_j \cdot \mathrm{ABSORB} \cdot \mathrm{COS}_{ijk},$$

where ϕ_{ijk} is the thermal flux density $(\mathrm{W \cdot m^{-2}})$ absorbed by a midelement inclined at inclination angle k from source sector i in hemispherical band j, and ABSORB is the thermal absorption coefficient which equals the emissivity at steady state.

The above assumes that there exist a single layer and a removed single midelement receiving flux from that layer. However, the contribution of absorbed thermal flux density from all hemispherical sectors, both upward and downward directions for each canopy layer, the sky, and ground, to each layer's midelements must be calculated (Fig. 4). The calculations should account for the fact that within each sector the flux which originates from any given layer is obstructed by other elements before the flux reaches any specified midelement in another layer. In addition, a relatively large number of permutations must be calculated, since each layer is simultaneously emitting thermal flux to other layers and absorbing emitted flux from the surrounding leaves, other layers, the sky, and the ground. For each permutation a contribution coefficient which replaces PHIT_j is calculated. For example, the midelements in layer 1 will receive thermal flux from the sky, layer 1, layer 2, layer 3, and the ground. For all sectors defined within a specific hemispherical band j, the contributing coefficients are calculated as follows.

The proportion of sky thermal flux within a sector in band j reaching the midelements in layer 1 is PGAP_{j1}. The contributing coefficient from layer 1 to the layer 1

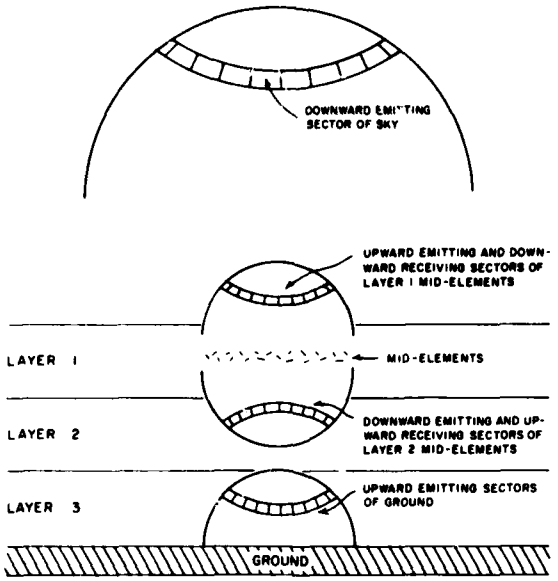

Fig. 4. Hemispherical sectors are shown for the sky, layer 1, and the ground. Note only sectors in one band are shown.

midelements is $2 \cdot (\mathrm{PHIT}'_{j1})$. The coefficient of 2 accounts for the two half-layers comprising layer 1. The contributing coefficient from layer 2 to the layer 1 midelements can be derived in the following manner. The probability of gap to layer 2 is PGAP'_{j1}. Once layer 2 is reached, the projected surface area of interest is PHIT_{j2}. Thus the contributing coefficient is $\mathrm{PGAP}'_{j1} \cdot \mathrm{PHIT}_{j2}$. A similar argument can be made for the contributing coefficient from layer 3 to the layer 1 midelements $\mathrm{PGAP}'_{j1} \cdot \mathrm{PGAP}_{j2} \cdot \mathrm{PHIT}_{j3}$. The contributing coefficient from the ground to layer 1 midelements is $\mathrm{PGAP}'_{j1} \cdot \mathrm{PGAP}_{j2} \cdot \mathrm{PGAP}_{j3}$. The contributing coefficients for both upward and downward directions of a particular sector and layer should sum to 2.0 representing the two sides of the midelements. And, in fact, if one sums the above coefficients, the total is 2.0. In a similar fashion, the contributing coefficients from all source sectors to layers 2 and 3 midelements are calculated.

Incorporating this information the equation is

$$\frac{\Phi_{ijklm}}{m^2} = M_l \cdot \mathrm{CONT}_{jlm} \cdot \mathrm{SECTOR}_j \cdot \mathrm{ABSORB}_m \cdot \mathrm{COS}_{ijk}.$$

where

Φ_{ijklm/m^2} = the thermal flux density absorbed by a midelement in layer m inclined at inclination angle k. The flux originates from emitting elements in layer l and is contained within sector i in hemispherical band j. Note that the index l represents the sky and ground in addition to the three canopy layers.

M_l = average thermal exitance of elements in layer l.

CONT_{jlm} = contributing coefficient for midelements in layer m absorbing flux from elements in layer l for all sectors within hemispherical band j; and

ABSORB_m = average thermal absorption coefficient for elements in layer m.

Except for the sky thermal exitance, M_l can be further expressed in terms of the Stefan-Boltzmann law in terms of ϵ_l, the average emissivity of elements in layer l, and T_l, the true average surface temperature (K) of the midelements in layer l (unknown). Note that the average surface temperatures of the three canopy midelements are not known, and these values must be derived mathematically. In addition, the ground temperature is known (input), and the sky exitance is calculated by an empirical equation as a function of air temperature (input). Thus the final equation becomes

$$\frac{\Phi_{ijklm}}{m^2} = \sigma \cdot \epsilon_l \cdot T_l^4 \cdot \mathrm{CONT}_{jlm} \cdot \mathrm{SECTOR}_j \cdot \mathrm{ABSORB}_m \cdot \mathrm{COS}_{ijk}.$$

The total flux density emitted by elements in layer l and absorbed by a particular midelement in layer m at inclination k can be described by

$$\frac{\Phi_{klm}}{m^2} = \sigma \cdot \epsilon_l \cdot T_l^4 \cdot \mathrm{ABSORB}_m \cdot \sum_{j=1}^{9} \mathrm{CONT}_{jlm} \cdot \mathrm{SECTOR}_j \cdot \left(\sum_{i=1}^{18} \mathrm{COS}_{ijk} \right).$$

The total flux density absorbed by a midelement in layer m at inclination angle k is computed by summing all sources:

$$\frac{\Phi_{km}}{m^2} = \sum_{l=1}^{5} \frac{\Phi_{klm}}{m^2},$$

where $l = 1, 2, 3, 4, 5$ represents the sky, layer 1, layer 2, layer 3, and the ground, respectively.

Nine equations for each layer are constructed. Each equation represents the absorbed flux density for each midelement inclination. For each layer the appropriate equation is weighted by the frequency of occurrence of the elements within the corresponding inclination class. The nine equations are then summed to represent the average absorbed thermal flux density within the three canopy layers. In addition, the flux density absorbed ($\mathrm{W/m^2}$) is on a per unit area basis. Thus the $\mathrm{m^2}$ term above must represent both the top and bottom surfaces of the leaf. As a consequence, the factor of $1/2$ is introduced:

$$\frac{\Phi_m}{m^2} = \frac{1}{2} \sum_{k=1}^{9} \frac{\Phi_{km}}{m^2} \cdot \mathrm{FREQD}_{km},$$

where Φ_m/m^2 is the average absorbed thermal flux density by the midelements in layer m, and FREQD_{km} is the probability of occurrence of inclination k for elements in layer m. The resulting three equations represent the average absorbed thermal flux density for each layer. To complete the energy budget for each layer we must include absorbed solar radiation, convection, transpiration, and thermal radiant emission.

D. Solar Radiation Absorption

Several models have been developed to study the interactions of solar radiation within vegetation canopies. Allen and Richardson,[28] Alderfer and Gates,[29] and Suits[30] have adapted a system of simultaneous differential equations developed by Kubelka and Munk[31] in various ways to vegetation canopies. Suits[30] developed a model which includes geometric effects and predicts non-Lambertian characteristics of vegetation canopies. Chance and LeMaster[32] have derived a light absorption model for vegetative plant canopies from the Suits reflectance model.

Another approach, developed by Smith and Oliver,[33] is the Solar Radiation Vegetation Canopy (SRVC) model. The model is stochastic in nature and predicts the diurnal apparent directional spectral reflectance of a vegetation canopy. The same canopy geometry as described above is utilized within the SRVC model. This model was modified to predict the average absorbed solar radiation within each canopy layer as described by Kimes.[19] Although the SRVC absorption model was used exclusively in this study, any desirable solar absorption model which predicts the proportion of absorbed spectral solar irradiance in a canopy layer could be utilized.

E. Other Energy Transfers

The remaining energy transfers to and from the midelements include thermal exitance, transpiration, and convection. The thermal exitance $M(\mathrm{W \cdot m^{-2}})$ of all midelements in layer l is calculated by the Stefan-Boltzmann law:

$$M_l = \sigma \cdot \epsilon_l \cdot T_l^4,$$

where σ is the Stefan-Boltzmann constant $(\mathrm{W \cdot m^{-2} \cdot K^{-4}})$, ϵ_l is the emissivity of midelements in layer l (input), and T_l is the mean surface temperature of midelements in layer l(K). The ground thermal exitance is calculated in a similar fashion.

A number of transpirational and convectional formulations can be utilized within the model. In light of the fact that the model was to be validated on a lodgepole pine stand, the following transpirational and convectional equations were incorporated. Gates[8] presented the equation used for transpiration, which was later discussed by Lee and Gates[34] in detail. The water vapor density within the leaf is assumed to be at saturation at the leaf temperature. The equation for any particular midleaf is

$$\mathrm{TRANS}_l = H(T_l)\left[\frac{s\rho l(T_l) - \mathrm{RH} \cdot s\rho a(T_a)}{R_l + R_a}\right](697.8),$$

where

TRANS_l = transpirational loss from leaf in layer $l(\mathrm{W \cdot m^{-2}})$;

$H(T_l)$ = latent heat of vaporization of water at the leaf temperature $T_l(\mathrm{cal \cdot g^{-1}})$;

$s\rho l(T_l)$ = water vapor density inside the leaf at saturation at the leaf temperature $T_l(\mathrm{g \cdot cm^{-3}})$;

RH = relative humidity of air (input);

$s\rho a(T_a)$ = water vapor density at saturation of the free air beyond the boundary layer of the leaf at the air temperature $T_a(\mathrm{g \cdot cm^{-3}})$;

R_l = internal leaf resistance to water vapor diffusion in $\mathrm{min \cdot cm^{-1}}$ (input); and

R_a = resistance of the boundary layer to water vapor diffusion $(\mathrm{min \cdot cm^{-1}})$.

$H(T_l)$, $s\rho l(T_l)$, and $s\rho a(T_a)$ were calculated using physically based formulas. Values of R_a for lodgepole pine needles were estimated from a mass transfer determination of Landsberg and Ludlow[35] who used Sitka spruce shoots. The formula is $R_a = [0.04 + 1.27(\mu^{-0.5})]/60$, where μ is the wind speed in $\mathrm{cm \cdot sec^{-1}}$ (input).

The constant R_l value used for the lodgepole pines in this study was 0.66 min/cm. Gates[36] and Miller and Gates[37] reported R_l values of 0.72, 0.33, and 0.50 min/cm for *Picea mariana*, *Pinus resinosa*, and *Pinus strobus*, respectively. Jarvis *et al.*[38] and Tenhunen and Gates[39] presented recent investigations of the stomatal opening and closing as influenced by environmental factors and concluded that the complex control of the stomata has not yet been described adequately.

The following convection equation was utilized. Tibbals *et al.*[40] conducted quantitative measurements on silver castings of blue spruce and white fir branches in a controlled radiation and wind tunnel chamber. The authors report convective coefficients for free convection in both species. However, Gates[8] notes that rarely in nature is there any air movement $<8.8\ \mathrm{cm \cdot sec^{-1}}$ (0.2 mph). As a consequence, an equation describing forced convection can be used to approximate all convectional exchanges. Tibbals *et al.*[40] found that both longitudinal and horizontal wind flows gave equal coefficients for spruce:

$$\text{For } \mu > 30.0 \quad h_c = (0.95\mu^{0.97}) \cdot (0.698),$$

$$\text{For } \mu < 30.0 \quad h_c = (20.4 + 0.2\mu^{0.97}) \cdot (0.698),$$

where μ is the wind velocity in $\mathrm{cm \cdot sec^{-1}}$ (input), and h_c is the convectional coefficient in $\mathrm{W \cdot m^{-2} \cdot {}^{\circ}C^{-1}}$.

The convectional exchange of a midelement is calculated as $Q_{FC} = h_c \cdot (T_s - T_a)$, where Q_{FC} is the power per unit area of midelement loss or gain $(\mathrm{W \cdot m^{-2}})$, T_s is the surface temperature of the midelement in °C, and T_a is the air temperature of the free air beyond the boundary layer in °C (input).

The sky thermal exitance was calculated by an empirical equation dependent only on air temperature near the ground surface, and clear sky conditions were assumed.[9] Hudson[20] presented several references which estimate sky thermal exitance in a similar manner.

It is important to note that a multitude of convectional, transpirational, sky thermal exitance, and solar absorption formulations exist that may be more suitable for specific modeling objectives. For this reason the model has been structured so that different formulations of the above can be easily incorporated within the model.

F. Model Solution

The total energy budget equations for each canopy layer are formed, and the result is a system of three nonlinear equations and three unknowns. The three unknowns are the surface temperature of the midelements in each layer, which represent the respective average temperature of each layer:

$$\mathbf{F} = \begin{bmatrix} \text{layer 1 energy budget equation} \\ \text{layer 2 energy budget equation} \\ \text{layer 3 energy budget equation} \end{bmatrix} = \tilde{0}.$$

To solve this system of equations the model calls the ZSYSTM algorithm from the International Mathematical and Statistical Library.[41] The roots of the system predict the average temperature of the layers and are used to calculate the following thermal predictions.

G. Thermal Predictions

The model predicts the thermal radiance, effective radiant temperature (ERT), and equivalent exitance in the nine viewing inclination bands at 10° intervals above the canopy. The contribution of each canopy layer and the ground to the nine sensing positions are calculated as follows. The thermal radiance in the band direction j is

$$\begin{aligned} L_j = \pi^{-1} \cdot (&\mathrm{PHIT}_{j1} \cdot \epsilon_1 \cdot \sigma \cdot X_1^4 \\ &+ \mathrm{PGAP}_{j1} \cdot \mathrm{PHIT}_{j2} \cdot \epsilon_2 \cdot \sigma \cdot X_2^4 \\ &+ \mathrm{PGAP}_{j1} \cdot \mathrm{PGAP}_{j2} \cdot \mathrm{PHIT}_{j3} \cdot \epsilon_3 \cdot \sigma \cdot X_3^4 \\ &+ \mathrm{PGAP}_{j1} \cdot \mathrm{PGAP}_{j2} \cdot \mathrm{PGAP}_{j3} \cdot \epsilon_4 \cdot \sigma \cdot X_4^4), \end{aligned}$$

where each term on the right-hand side of the equation represents the thermal radiance contribution to the sensor by layer 1, layer 2, layer 3, and layer 4 (ground), respectively; L_j is the thermal radiance at viewing angle j($\mathrm{W \cdot m^{-2} \cdot sr^{-1}}$); and X_m is the average surface temperature of elements in layer m(K), m = 1,2,3,4.

The thermal radiance L_j can be converted to the equivalent exitance M_j by $M_j = L_j \cdot \pi$, and the effective radiant temperature (ERT_j K) in band direction j can be calculated as $\mathrm{ERT}_j = (M_j/\sigma)^{1/4}$, where σ is the Stefan-Boltzmann constant.

The model also predicts the ERT in the horizontal direction from the ground for each of the three layers. When looking horizontally at a canopy the probability of gap is 0.0 according to the assumptions in the model. Thus for a relatively narrow field of view the horizontal looking ERT of any given layer is calculated by using the Stefan-Boltzmann equation with the appropriate emissivity factor and average layer temperature.

III. Field Measurements and Simulation

A unique thermal and environmental data base for a lodgepole pine canopy at Leadville, Colo. was collected during 1977. Four clustered lodgepole pine trees were chosen for intensive study. These modeling trees had the following mean statistics: 6.0-m height; 30-year age; 13.2-cm DBH; and a surrounding stand of 102-$\mathrm{m^2}$/ha basal area. The S parameter, foliage area indices, and foliage angle frequency distributions of the modeling canopy were measured as reported by Kimes *et al.*[42]

Personnel from the Army Corps of Engineers Waterways Experiment Station, Environmental Laboratory (WES/EL) at Vicksburg, Miss. developed a system for automated collecting, processing, and displaying environmental baseline data as described by West and Floyd.[43] The system was utilized to monitor environmental conditions at the study site for July, September, and October 1977. All sensor measurements were recorded once very hour continuously for the duration of the study. The measurements taken included air temperature, global solar irradiance, wind speed, wind direction, rainfall, relative humidity, soil temperature, and vegetation surface temperature. The specific make and calibration procedures of the above instrumentation are described by West and Floyd.[43]

The environmental measurements used as model inputs for the reported validation are as follows. Global solar irradiance was measured in a meadow clearing. Air temperature was measured 1 m above the ground in the middle of the four modeling trees. Wind speed and relative humidity were measured 1 m above the ground in the surrounding canopy. Ground temperature was measured by contact thermistors placed on the ground surface.

In addition, the Wahl Digital Heat Spy-DSH-14 Thermal Radiometer with a bandpass of 4.8–20.0 m and a 3.5° field of view was used to measure the average horizontal ERT of layer 2 of the canopy at four stake positions. The four stakes circumvent the west semicircle of the modeling trees and were ~4.5 m from the

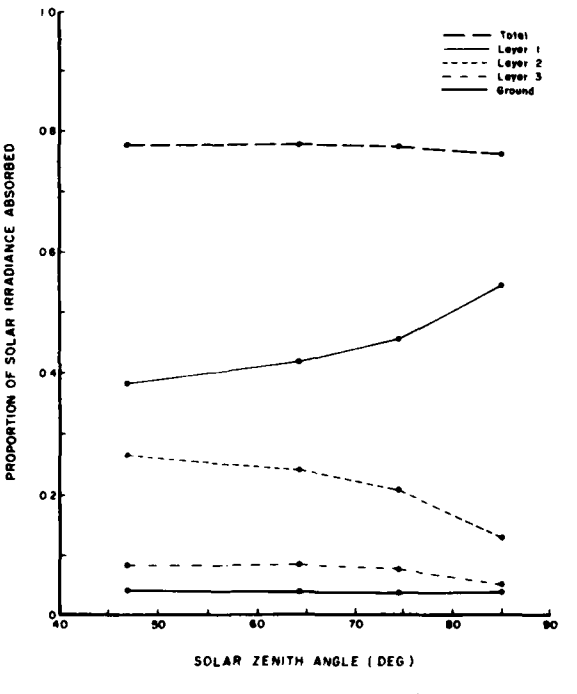

Fig. 5. Simulated proportion of global solar irradiance absorbed by the lodgepole pine canopy system (total), layer 1, layer 2, layer 3, and the ground as a function of solar zenith angle.

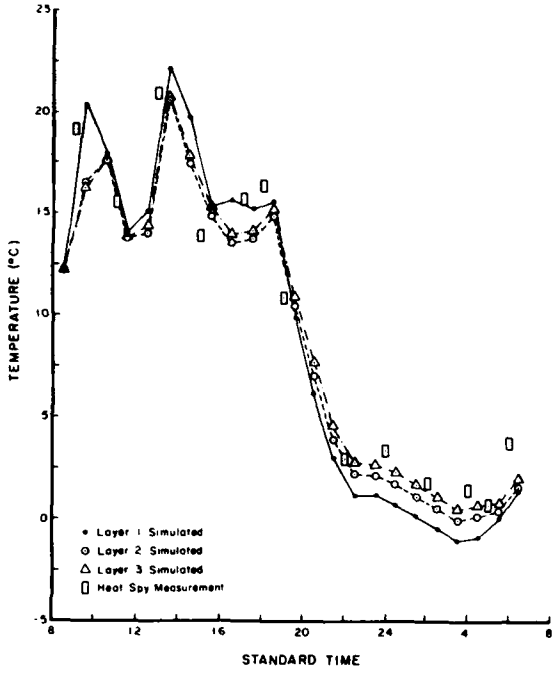

Fig. 6. Simulated vs measured lodgepole pine canopy horizontal ERTs for 15–16 July 1977. Measured ERTs are the mean of four horizontal ERTs of the middle layer as measured by the Wahl Heat Spy.

center of the modeling tree clusters. At this distance the field of view of the Heat Spy was averaged over a large number of canopy elements.

The SRVC absorption model[19] was used to simulate the spectral solar absorption in the three layers of the modeling canopy for the 15–16 July 1977 diurnal cycle.

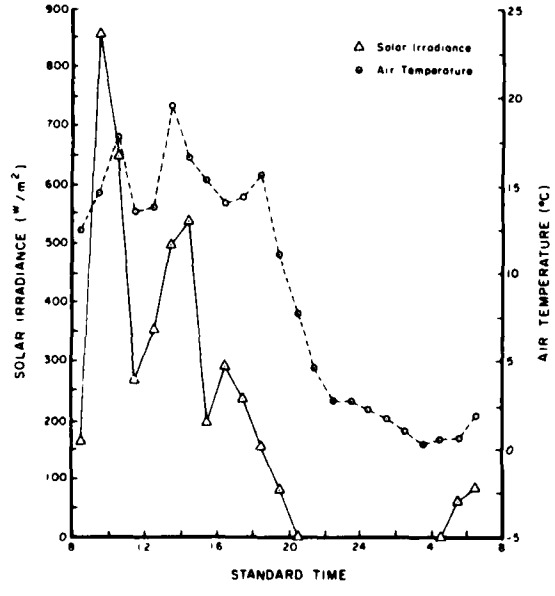

Fig. 7. Measured global solar irradiance and air temperature for 15–16 July 1977.

In this study the thermal behavior of the lodgepole pine canopy was simulated for the 15–16 July 1977 diurnal cycle. The mean of the four horizontal Heat Spy ERTs was used to test the model's accuracy of prediction. Other validations, sensitivity analyses, and error analyses of the model for the lodgepole pine canopy were reported by Kimes.[19]

IV. Results and Discussion

The results from the SRVC absorption model showed that the total global irradiance absorbed by the lodgepole pine canopy system was relatively constant with solar zenith angle. However, the proportion of total global irradiance absorbed by individual canopy layers varied as a function of solar zenith angle (Fig. 5). The mean total solar flux absorbed per unit canopy element surface area for any given layer and solar zenith angle was calculated from the information in Fig. 5 as presented by Kimes.[19]

The simulated horizontal ERTs for the three layers for 15–16 July are presented in Fig. 6 along with the mean of the four horizontal Heat Spy ERTs. The corresponding measured solar irradiance and air temperature are presented in Fig. 7. During the 1630 and 0530 standard times, the relative humidity was at a minimum (0.06) and maximum (0.85), respectively. Wind speed was 0.0 m/sec for all measurement periods; the minimum recorded wind speed possible was 10 cm/sec. Gates[8] stated that rarely is wind speed in natural environments below 8 cm/sec. As a consequence, for periods when wind speed was recorded to be 0.0, a minimum value of 10 cm/sec was utilized. It should be noted that the simulated data were derived from the meteorological data which were recorded at hourly intervals, and the Heat Spy measurements were not necessarily synchronous in time. Consequently, one must compare the general trends of the simulated data to the Heat Spy measurements. In fact, the erratic nature of the solar irradiance (Fig. 7) suggests that between hourly intervals, the true solar irradiance function could vary widely. This fact could explain some of the deviations during the day shown in Fig. 6. During the night the simulated values deviated from the measured temperature by <1.5°C.

Selected output for 0930 and 0330 (Standard Time) simulations is presented in Table I. During the day the average layer temperature decreases as one proceeds from layer 1 to layer 3 due to solar heating and canopy geometry interactions. During the nighttime, however, the layers cool differentially due to the relatively low thermal exitance of a clear sky and the relatively high surface temperature of the ground. As a consequence, layer 3 has the highest temperature. These trends are documented by Geiger.[44]

The ERT perceived by a sensor above the canopy as a function of view angle is dependent on the above layer temperature differentials and the canopy geometry (Table I). At the lowest sensor inclination angles, the ERT strongly reflects the temperature of layer 1. As

Table I. Selected Output for 0930 and 0330 (Standard Time) 15–16 July 1977

Time = 0930
Average element temperatures (layers 1–3) = 20.4, 16.6, 16.3°C
The thermal exitance and ERT above the canopy for the various viewing angles are:

Inclination (deg)	Exitance (W/m²)	ERT (°C)
5	419	20.3
15	413	19.2
25	410	18.6
35	408	18.4
45	408	18.2
55	407	18.1
65	407	18.1
75	407	18.1
85	407	18.1

Time = 0330
Average element temperatures (layers 1–3) = −1.0, −0.0, 0.5°C
The thermal exitance and ERT above the canopy for the various viewing angles are:

Inclination (deg)	Exitance (W/m²)	ERT (°C)
5	310	−1.0
15	311	−0.6
25	313	−0.4
35	314	−0.2
45	314	−0.1
55	314	−0.1
65	315	−0.1
75	315	−0.1
85	315	−0.1

the sensor view inclination angle increases, the second, third, and ground layer temperatures more strongly influence the sensor ERT. Kimes[19] has shown that particular canopy geometries (leaf angle distribution, leaf area index, and leaf spatial distributions) can have very significant effects on the simulated ERT of the sensor at varying view angles, and this phenomenon suggests important implications on the optimum view angle for making inferences about the target of interest. These relationships have been further explored for wheat canopies as reported by Kimes *et al.*[45]

To recapitulate, a model incorporating the geometric structure of a vegetation canopy and predicting the thermal response of the canopy under various environmental conditions was developed. The model is designed to be instantaneous in nature, e.g., all canopy elements are under steady-state conditions, and no heat storage may occur. Therefore, the model is independent of all previous environmental events. In many applications of the model this feature would be highly desirable (e.g., when the environmental history is not known). However, to approximate the time-dependent phenomena (nonsteady-state conditions), one can use a series of incremental changes of steady-state energy flows.[13] In branches and boles a significant amount of heat storage and conduction may be operating, and the above modifications may be desirable in some applications.

The model was applied to a lodgepole pine canopy. The algorithms incorporated for transpiration and convection were rather simplistic in their assumptions. For example, the constant R_l parameter used in this study is actually variable in lodgepole pine and is dependent on complex soil–plant water relationships.[46,47] One of the greatest barriers in applying a model to a variety of vegetation species and obtaining accurate results is the physiological diversity of different species and the fact that the physiological response of many species are not understood sufficiently to be predictable.[48]

The model validation presented is by no means comprehensive. The simulated and measured lodgepole pine canopy temperatures closely followed air temperatures; the close agreement in this instance may be fortuitous and could be quite different under various vegetation canopy structures, plant–water relations, and environmental conditions. The emphasis of the model presented is on assessing the form of radiant transfers in vegetation canopies and to provide a mathematical framework for incorporating all the energy transfer processes within a canopy. Depending on the researcher's knowledge of the vegetation canopy of interest and his modeling criteria, more appropriate energy transfer algorithms (e.g., transpiration and convection) can be incorporated in the present model.

V. Conclusions

The thermal IR exitance model provides a framework for simulating energy transfers within vegetation canopies of specific geometric structures. The model is unique in that it incorporates the geometric canopy structure to define the radiant transfer functions within and above the canopy systems. It predicts the average surface temperature of canopy layer elements and the response of a thermal IR sensor above the canopy as a function of view angle.

The model was shown to couple successfully the environmental factors and the geometric and physical

factors of canopy elements to predict the average canopy element temperatures for a lodgepole pine canopy. During the July simulation the differentials between the simulated vs measured horizontal effective radiant temperatures for a lodgepole pine canopy were, in general, <2°C.

Simulated results suggested that for certain canopy element inclination distributions, canopy LAI, and environmental conditions, the sensor inclination angle will greatly affect the sensor response; and this phenomenon has important implications on the optimum view angle for making inferences about the target of interest.

Model simulations showed that the total global irradiance absorbed by the lodgepole pine canopy system is relatively constant with solar zenith angle. However, the proportion of total global irradiance absorbed by individual canopy layers varied as a function of solar zenith angle.

The model provides a modeling framework which may be useful to a variety of research interests. Specific energy transfer algorithms, which are best suited to the researcher's modeling criteria, can be incorporated.

This work was carried out at Colorado State University and sponsored by the U.S. Army Research Office with grant DAAG 29-78-0045 and, in part, by the U.S. Army Engineers Waterways Experiment Station with contract DACW-39-77-C-0073. D. S. Kimes received the degree of Doctor of Philosophy from Colorado State University in part for the work reported here.

References

1. R. A. Holmes and R. B. MacDonald, Proc. IEEE **57**, 629 (1969).
2. D. A. Landgrebe, L. L. Biehl, and W. S. Simmons, IEEE Trans. Geosci. Electron. **GE-15**, 120 (1977).
3. L. A. Bartolucci, P. H. Swain, and C. Wu, IEEE Trans. Geosci. Electron. **GE-14**, 101 (1977).
4. A. Kahle, J. Geophys. Res. **83**, 1673 (1977).
5. K. Watson, L. E. Rowan, and T. W. Offield, at Seventh Symposium on Remote Sensing of the Environment, U. Michigan, Ann Arbor (1971), p. 2017.
6. K. Watson, in *NASA Third Annual Earth Resources Aircraft Program Review*, (NASA, Houston, 1971).
7. U. Michigan, "Target Temperature Modeling," Evaluation of contract F30602-68-C-099, Defense Documentation Center (1969).
8. D. M. Gates, *Energy Exchange in the Biosphere* (Harper and Row, New York, 1968).
9. D. S. Kimes, K. J. Ranson, J. A. Kirchner, and J. A. Smith, "Modeling Descriptions and Terrain Modules," Final Report under contract DACW-39-77-C-0073 (Colorado State U., Fort Collins, 1978).
10. J. A. Wiebelt and J. B. Henderson, "Techniques and Analysis of Thermal Infrared Camouflage in Foliated Backgrounds," Final Report under contract DAAG53-76-C-0134 (Oklahoma State U., Stillwater, 1977).
11. J. L. Heilman, E. T. Kanemasu, and N. J. Rosenberg, Remote Sensing Environ. **5**, 137 (1976).
12. J. A. Smith and R. E. Oliver, Appl. Opt. **13**, 1599 (1974).
13. D. M. Gates, in *Perspectives of Biophysical Ecology*, D. M. Gates and R. B. Schmerl, Eds. (Springer, Berlin, 1974), pp. 1–28.
14. K. Ya. Kondratyev, "Actinometry," contract NASA TT F-9712 (NASA, Washington, D.C., 1965).
15. V. Leeman, D. Earing, R. K. Vincent, and S. Ladd, "The NASA Earth Resources Spectral Information System: A Data Compilation," contract NASA CR-WRL-31650-T (U. Michigan, Ann Arbor, 1971).
16. J. Ross, in *Vegetation and the Atmosphere: Vol. 1, Principles*, J. L. Monteith, Ed. (Academic, New York, 1976).
17. K. L. Blaxter, *The Energy Metabolism of Ruminants* (Hutchinson, London, 1967).
18. S. B. Idso, R. D. Jackson, W. L. Ehrler, and S. T. Mitchell, Ecology **50**, 899 (1969).
19. D. S. Kimes, "A Thermal Vegetation Canopy Model of Sensor Responses," Ph.D. Dissertation, Colorado State U., Fort Collins (1979).
20. R. D. Hudson, Jr., *Infrared System Engineering* (Wiley, New York, 1969).
21. J. L. Monteith, Ann. Bot. London **29** (133), 17 (1965).
22. J. W. Wilson, J. Appl. Ecol. **2**, 383 (1965).
23. C. T. de Wit, "Photosynthesis of Leaf Canopies," Agricultural Research Report 663, Wageningen, Netherlands (1965).
24. T. Nilson, Agric. Meteorol. **7**, 25 (1970).
25. S. B. Idso and C. T. de Wit, Appl. Opt. **9**, 177 (1970).
26. R. E. Oliver and J. A. Smith, "A Stochastic Canopy Model of Diurnal Reflectance," Final Report under contract DAH C04-74-60001 (Durham, N.C., 1974).
27. F. E. Nicodemus *et al.*, Self-Study Manual on Optical Radiation Measurements, Parts 1, 2, 3, (National Bureau of Standards, Institute for Basic Standards, Washington, D.C., 1978).
28. W. A. Allen and J. A. Richardson, J. Opt. Soc. Am. **58**, 1023 (1968).
29. R. G. Alderfer and D. M. Gates, Ecology **52**, 855 (1971).
30. G. H. Suits, Remote Sensing Environ. **2**, 177 (1972).
31. P. Kubelka and F. Munk, Z. Tech. Phys. **11**, 593 (1931).
32. J. E. Chance and E. W. LeMaster, Appl. Opt. **17**, 2629 (1978).
33. J. Smith and R. E. Oliver, at Eighth Symposium on Remote Sensing of the Environment, U. Michigan, Ann Arbor (1972), pp. 1333–1353.
34. R. Lee and D. M. Gates, Am. J. Bot. **15**, 963 (1964).
35. J. J. Landsberg and M. M. Ludlow, J. Appl. Ecol. **7**, 187 (1969).
36. D. M. Gates, Q. Rev. Biol. **41**, 363 (1966).
37. P. Miller and D. M. Gates, Am. Midl. Nat. **77**, 77 (1967).
38. P. G. Jarvis, G. B. James, and J. J. Landsberg, in *Vegetation and the Atmosphere: Vol. 2, Case Studies*, J. L. Monteith, Ed. (Academic, New York, 1976), pp. 171–240.
39. J. D. Tenhunen and D. M. Gates, in *Perspectives of Biophysical Ecology*, D. M. Gates and R. B. Schmerl, Eds. (Springer, New York, 1975).
40. E. C. Tibbals, E. K. Carr, D. M. Gates, and F. Kreith, Am. J. Bot. **51**, 529 (1964).
41. IMSL Library 3, Edition 5 (Fortran) CDC 6000/7000, CYBER 70/170 Series (International Mathematical and Statistical Libraries, 1977).
42. D. S. Kimes, J. A. Smith, and J. K. Berry, Aust. J. Bot. **27**, 575 (1979).
43. H. W. West and H. M. Floyd, "An Automated System for Collecting Processing and Displaying Environmental Baseline Data," Technical Report M-76-11, U.S. Army Engineer Waterways Experiment Station, Vicksburg, Miss. (1976).
44. R. Geiger, *The Climate Near the Ground* (Harvard U. P., Cambridge, Mass., 1965).
45. D. S. Kimes, S. B. Idso, P. J. Pinter, Jr., R. D. Jackson, and R. J. Reginato, Rem. Sens. Env. in press (1981).
46. S. W. Running, in *Proceedings, Fourteenth Conference on Agriculture and Forest Meteorology* (American Meteorological Society, Boston, 1978).
47. G. F. Byrne, J. E. Begg, P. M. Fleming, and F. X. Dunin, Remote Sensing Environ. **8**, 291 (1979).
48. T. M. Hinckley, J. P. Lassoie, and S. W. Running, For. Sci. Monogr. 20 (1978).